

On the approximation of queue-length distributions in transportation networks

Jing Lu

Operations Research Center
Massachusetts Institute of Technology, USA
Email: jl3724@mit.edu

May 19, 2021

Abstract

This paper focuses on the analytical probabilistic modeling of vehicular traffic. It formulates a stochastic node model. It then formulates a network model by coupling the node model with the link model of Lu and Osorio (2018), which is a stochastic formulation of the traffic-theoretic link transmission model. The proposed network model is scalable and computationally efficient, making it suitable for urban network optimization. For a network with r links, each of space capacity ℓ , the model has a complexity of $\mathcal{O}(r\ell)$. The network model yields the marginal distribution of link states. The model is validated versus a simulation-based network implementation of the stochastic link transmission model. The validation experiments consider a set of small network with intricate traffic dynamics. For all scenarios, the proposed model accurately captures the traffic dynamics. The network model is used to address a signal control problem. Compared to the probabilistic link model of Lu and Osorio (2018) with an exogenous node model and a benchmark deterministic network loading model, the proposed network model derives signal plans with better performance. The case study highlights the added value of using between-link (i.e., across-node) interaction information for traffic management and accounting for stochasticity in the network.

1 Introduction

This paper formulates an analytical stochastic (i.e., probabilistic) network model. It formulates a node model, and couples the node model with an existing stochastic link model. Our focus on stochastic analytical modeling is motivated by an interest in developing macroscopic traffic models that can both provide a more detailed distributional description of network performance and can be used for large-scale network analysis and optimization. The increase in the

quantity, quality and resolution of traffic data available allows to validate models that provide a probabilistic description of traffic. Such models can be used to enhance the reliability and the robustness of our transportation networks. Major agencies in the US and in Europe are focusing on measuring and improving such reliability and robustness performance metrics. Our research in probabilistic network modeling is to formulate traffic models that are suitable for the efficient analysis and optimization of large-scale networks.

A stochastic network model consists of two main components: a link model, which describes traffic dynamics within a homogeneous road segment, and a node model, which describes traffic dynamics between links. There is an increasing and recent interest in the formulation of probabilistic traffic-theoretic link models. Recent reviews include Jabari (2012) and Laval and Chilukuri (2014). Probabilistic link model formulations with traffic-theoretic foundations include Boel and Mihaylova (2006); Sumalee et al. (2011); Jabari and Liu (2012, 2013); Osorio et al. (2011); Deng et al. (2013); Laval and Chilukuri (2014); Laval and Castrillón (2015); Osorio and Flötteröd (2015); Lu and Osorio (2018); Lu (2020). The main approaches have been the introduction of randomness in the cell transmission model, extensions of the variational theory of Daganzo (2005) and the use of probabilistic queueing theory (Olszewski, 1994; Heidemann, 2001; Viti and Van Zuylen, 2010; Osorio et al., 2011; Osorio and Flötteröd, 2015; Lu and Osorio, 2018). Another stream of research in the estimation of queue length distribution is based on observed data collected from probe vehicles (Comert and Cetin, 2009, 2011; Comert, 2013, 2016).

The model of Osorio and Flötteröd (2015) is a queueing-theoretic model that is a stochastic formulation of the deterministic link-transmission model of Yperman et al. (2007), which itself is an operational formulation of Newell’s simplified theory of kinematic waves (Newell, 1993). For a link with space capacity ℓ , the model complexity is in the order of $\mathcal{O}(\ell^3)$. Lu and Osorio (2018) have extended the formulation of Osorio and Flötteröd (2015), leading to a model with complexity in the order of $\mathcal{O}(\ell)$. This is a formulation that scales linearly with the link’s space capacity, making it efficient and appropriate for large-scale network analysis. The work of Chapter 3 of Lu (2020) further reduces the model complexity to a constant that no longer depends on the link’s space capacity. This makes the proposed model suitable for large-scale network optimization or situations where a large number of model evaluations is required. In this paper, we focus on the network model development with the analytical probabilistic link model of Lu and Osorio (2018) where the transient distribution of the queue-length is produced.

The formulation of traffic-theoretic node models is limited to deterministic formulations (e.g., Daganzo (1995); Lebacque (1996, 2005); Corthout et al. (2012); Flötteröd and Rohde (2011); Tampère et al. (2011b); Smits et al. (2015)). These node models satisfy supply and demand restrictions at the link boundaries, mass balance requirements on flows across the node and some further considers the distribution of demands to different outgoing links to reflect destination desires of drivers. Most deterministic node models imposes flow maximization to facilitate the physical requirement that traffic-holding does not exist. It is shown in a recent work of Jabari (2016) that flow maximized solutions are only sufficient conditions for holding-free solutions, especially in complex congested urban intersections. Other themes of node modeling include the derivation of formulas for calculating node flows that satisfies the aforementioned restrictions (Bliemer, 2007). Nevertheless, one challenge of network modeling that persists today is the

analytically intractability due to the coupling with link dynamics and node models that are typically stated as optimization problems.

The development of stochastic node model is quite limited and mostly focused on tandem link, merge and divergence network topology. The model of Osorio et al. (2011) includes a stochastic node model for a simple two queue network. Osorio and Yamani (2017) proposes an analytical model to approximate the transient aggregate joint queue-length distribution of tandem links, the aggregation-disaggregation technique and network decomposition methods are used to reduce the model complexity. Osorio and Wang (2017) propose an analytical approximation of the aggregate stationary joint queue-length distributions for arbitrary size and it can be extended to general topology by coupling with the method introduced in Osorio and Bierlaire (2009). Flötteröd and Osorio (2017) develops an analytical stochastic link transmission model (SLTM) for networks that produces the transient joint queue-length distribution and demonstrated its usage on linear, diverge and merge node models within the SLTM framework. Nevertheless, there is a lack of stochastic node models that apply for general network topology and can be integrated with SLTM for marginal transient queue-length distribution for potentially large-scale network analysis.

In this article, we formulate a general stochastic node model that can be combined with various types of stochastic link models. We couple the proposed stochastic node model with the link model of Lu and Osorio (2018). Section 2 formulates the proposed stochastic network model. The model is validated in Section 3. It is used to address a signal control problem in Section 4. This case study shows the added value of accounting for between-link (i.e., across node) interactions for traffic management. Conclusions and a discussion of ongoing work are presented in Section 5.

2 Network model formulation

The proposed node model can be coupled with a variety of probabilistic link models to yield a network model. We present a general node model formulation. In this paper, we couple the node model with the link model of Lu and Osorio (2018), which produces the transient distribution of the link's queue length distribution. Section 2.1 briefly describes the link model, which is, hereafter, referred to as the mixture model. The node model formulation is given in Section 2.2.

2.1 Link model

We briefly outline here the main ideas of the link model of Lu and Osorio (2018). For a more detailed description, we refer the reader to Lu and Osorio (2018). The mixture model considers an isolated single-lane link. It assumes a triangular fundamental diagram. The link is parameterized as follows: free flow velocity v , backward wave speed w (negative), flow capacity \hat{q} , jam density $\hat{\rho}$, and link length L . The link model approximates the following process. Upon arrival to the link, vehicles are delayed L/v time units (known as the forward lag). After incurring this delay, vehicles are then ready for departure at the downstream end of the link.

Upon departure from the link, there is a delay of $L/|w|$ time units (known as the backward lag) before the newly available space is made available at the upstream end of the link. These delays or lags capture the time it takes forward, and backward, kinematic waves to traverse the link. The mixture model is a continuous-space discrete-time model. The lags are rounded to the nearest integer: $L/(v\delta)$ is rounded to k^{fwd} , and $L/(|w|\delta)$ is rounded to k^{bwd} , where δ is the incremental time.

The vehicular flow process described above is modeled with two queues. Vehicles that are ready for departure enter the *downstream queue*, denoted DQ . In other words, DQ captures the downstream boundary conditions of the link. Spaces that are occupied (i.e., they are either occupied by vehicles on the link, or by vehicles that have departed the link less than $L/(|w|\delta)$ time units ago) are represented by the *upstream queue*, denoted UQ . In other words, UQ captures the upstream boundary conditions of the link.

The the model of Lu and Osorio (2018) considers two univariate independent models: a univariate UQ model, which captures the link's upstream boundary conditions, and a univariate DQ model, which captures the link's downstream boundary conditions. Each of these two models approximates two distributions: (i) the distribution of the link's upstream queue UQ , and (ii) the distribution of the link's downstream queue DQ .

Then, the model of Lu and Osorio (2018) is defined as a mixture of these two models. For this discrete time model, let $UQ(k)$ denote the number of vehicles (or spaces occupied) in UQ at the end of discrete time interval k . We use similar notation for the downstream queue $DQ(k)$. The mixture model yields the marginal distributions of the downstream queue and of the upstream queue. These are given by:

$$P(UQ(k)) = \hat{w}P^{UQ}(UQ(k)) + (1 - \hat{w})P^{DQ}(UQ(k)) \quad (1)$$

$$P(DQ(k)) = \hat{w}P^{UQ}(DQ(k)) + (1 - \hat{w})P^{DQ}(DQ(k)), \quad (2)$$

where $P^{UQ}(UQ(k))$ (resp. $P^{DQ}(UQ(k))$) denotes the UQ distribution obtained from the univariate UQ (resp. DQ) model, $P^{UQ}(DQ(k))$ (resp. $P^{DQ}(DQ(k))$) denotes the DQ distribution obtained from the univariate UQ (resp. DQ) model, and \hat{w} denotes an exogenous weight parameter calculated according to Equation (37) of Lu and Osorio (2018).

The mixture model has linear complexity in the links space capacity ℓ because the two univariate models are independent. In other words, the distributions $P^{UQ}(UQ)$ and $P^{DQ}(UQ)$ are evaluated independently. Similarly, the distributions $P^{UQ}(DQ)$ and $P^{DQ}(DQ)$ are evaluated independently.

The stochastic processes that govern the link dynamics are as follows. The link is assumed to have an inhomogeneous Poisson arrival process with exogenous arrival rate $\lambda(k)$, and independent and exponentially distributed service times at the downstream end of the link with exogenous downstream flow capacity $\mu(k)$. It is shown in Chapter 3 section 3.4.2 of Lu (2020) that with proper time-varying arrival rate and service rate (i.e., $\lambda(k)$ and $\mu(k)$) and time increment δ , a link's boundary conditions for realistic traffic situation such as signalized links and

platoon arrival patterns can be estimated accurately compared to a details microscopic traffic simulator.

Each univariate model is then formulated as a system of nonlinear equations. For a given time interval k , the expected inflow into, and the expected outflow from, the link are assumed constant, and the solution of the system of nonlinear equations yields the transient (i.e., time-dependent) distribution of UQ (or of DQ) within the time interval k of duration δ . At the end of each time interval, the expected inflows and outflows are then updated and used for the next time interval.

2.2 Node model

We now formulate the node model. The analysis hereafter is for a given discrete time interval k . Hence, we use interchangeably UQ and $UQ(k)$, as well as DQ and $DQ(k)$. Consider a general node with m upstream links and n downstream links, let M be the set of upstream links and N be the set of downstream links. We assume exogenous turning probabilities $\{p_{ij}, i \in M, j \in N\}$. Each link i has an exogenous downstream flow capacity μ_i and space capacity ℓ_i . The rate at which vehicles can start trips at link i is exogenous and is denoted γ_i .

For a given upstream link i ($i \in M$), the number of vehicles ready for departure is DQ_i . For a given downstream link j ($j \in N$), the number of spaces available at the upstream end of link j (to accommodate demand from upstream links) is $(\ell_j - UQ_j)$.

We assume that a vehicle from i can transition to j if the following two conditions hold. First, the link j is not full so that there is space available to receive demand from upstream, i.e., $UQ_j < \ell_j$. Second, the vehicle is not blocked by vehicles in front that intend to leave link i to other downstream links other than link j . A sufficient, but not necessary, condition to ensure that vehicles from link i can transition to link j is that there is space available to receive vehicles in all downstream links, i.e., $\forall n \in N, UQ_n < \ell_n$. Additionally, if downstream links are not full, then the **instantaneous** departure rate from link i corresponds to its flow capacity, μ_i . This leads to the following expression for the expected flow rate from link i to link j during time interval k of length δ :

$$q_{i \rightarrow j}^{out}(k) = p_{ij} \mu_i P(DQ_i(k) > 0, UQ_n(k) < \ell_n \forall n \in N). \quad (3)$$

This proposed approximation may underestimate the true expected flow rate, since $\{DQ_i(k) > 0, UQ_n(k) < \ell_n \forall n \in N\}$ is a sufficient, but not a necessary, condition for flow transmission. For instance, there are cases where a downstream link is full, yet it does not hinder outflow from all upstream links. This can happen if there are no vehicles upstream that intend to enter the full downstream link. However, since it is assumed that there is always a constant non-zero proportion of outflows p_{ij} from upstream link i intent to enter the downstream link j that is full, link i will eventually be blocked, e.g., eventually the most downstreamed vehicle will become one that intends to join link j but not able to and hence blocked the outflow of the single-lane link i . The validation results of the next section indicate, this approximation has a minor effect on the accuracy of the model.

In order to combine the above expression with a link model requires the computation of the joint probability $P(DQ_i(k) > 0, UQ_n(k) < \ell_n \forall n \in N)$. In general, a straightforward, but also inefficient, way to compute this is to formulate a network model that jointly tracks the state of all links in the network. For a network with r links, each with space capacity ℓ , the model complexity would be in the order of $\mathcal{O}(\ell^r)$. Instead, we propose an approach with complexity $\mathcal{O}(r\ell)$. The main idea is to track the distribution of each link in the network independently, and to capture the dependencies between links by adjusting the arrival rates and the effective service rates of the links according to the expected flows within the network.

Section 2.2.1 formulates an approximation for the above joint probability, $P(DQ_i > 0, UQ_n < \ell_n \forall n \in N)$, which we refer to, hereafter, as the flow transmission probability. Section 2.2.2 then presents how the link model parameters (arrival rates and effective service rates) are approximated at every time step. Section 2.2.3 summarizes the method, and presents it as an algorithm.

2.2.1 Flow transmission probability

In this section, we present an analytical approximation of the flow transmission probability that only requires knowledge of the marginal univariate distributions of DQ and of UQ .

We use the inclusive-exclusive principle (Section 2.1 of Björklund et al. (2009)) to rewrite $P(DQ_i > 0, UQ_n < \ell_n \forall n \in N)$ as follows:

$$\begin{aligned}
P(DQ_i > 0, UQ_n < \ell_n \forall n \in N) &= & (4) \\
1 - P(DQ_i = 0) - \sum_{n \in N} P(UQ_n = \ell_n) \\
&+ \sum_{n \in N} P(DQ_i = 0, UQ_n = \ell_n) + \sum_{n \neq m; n, m \in N} P(UQ_n = \ell_n, UQ_m = \ell_m) \\
&+ \dots + (-1)^{|N|+1} P(DQ_i = 0, UQ_n = \ell_n \forall n \in N).
\end{aligned}$$

In Equation (4), the distribution of a single link state (e.g., $P(DQ_i = 0)$, $P(UQ_n = \ell_n)$) can be obtained directly from the link model. Let us now describe how we approximate the joint probabilities that appear in (4). Each joint probability is approximated by rewriting it as a conditional probability conditioned on the sum of the corresponding variables. For example:

$$\begin{aligned}
P(DQ_i = 0, UQ_n = \ell_n \forall n \in N) &= & (5) \\
&= P \left(DQ_i = 0, UQ_n = \ell_n \forall n \in N \mid DQ_i + \sum_{\forall n \in N} UQ_n = \sum_{\forall n \in N} \ell_n \right) \\
&\cdot P \left(DQ_i + \sum_{\forall n \in N} UQ_n = \sum_{\forall n \in N} \ell_n \right).
\end{aligned}$$

In order to derive an approximate expression for the right-hand side of Equation (5), we make two approximations. First, we approximate $DQ_i + \sum_{\forall n \in N} UQ_n$ as a Poisson arrival process

with rate $q(k)$. Hence,

$$P \left(DQ_i(k) + \sum_{\forall n \in N} UQ_n(k) = \sum_{\forall n \in N} \ell_n \right) = [\delta \cdot q(k)]^{\sum_{\forall n \in N} \ell_n} \frac{e^{-\delta \cdot q(k)}}{(\sum_{\forall n \in N} \ell_n)!}, \quad (6)$$

where δ is the time step length. The rate is given by the sum:

$$q(k) = q^{DQ_i}(k) + \sum_{\forall n \in N} q^{UQ_n}(k), \quad (7)$$

where $q^{DQ_i}(k)\delta$ (resp. $q^{UQ_n}(k)\delta$) represents the expected state of DQ_i (resp. UQ_n) for discrete time interval k . These can be obtained directly from the link model (see Equations (7) and (12) of Lu and Osorio (2018)). Let us briefly explain how they are calculated. The expression for $q^{UQ_n}(k)$ is:

$$q^{UQ_n}(k) = \sum_{r=0}^{k-1} q_n^{\text{in}}(r) - \sum_{r=0}^{k-k^{\text{bwd}}-1} q_n^{\text{out}}(r), \quad (8)$$

where $q_n^{\text{in}}(k)$ (resp. $q_n^{\text{out}}(k)$) denotes the instantaneous inflow (resp. outflow) rate of link n at the end of time interval k . This expression is obtained from the observation that the expected state of UQ_n represents the difference between the accumulated inflows to link n during the last $k - 1$ time steps and the accumulated outflows from link n during the last $k - k^{\text{bwd}} - 1$ time steps. Similarly, the expression for $q^{DQ_i}(k)$ is:

$$q^{DQ_i}(k) = \sum_{r=0}^{k-k^{\text{fwd}}-1} q_i^{\text{in}}(r) - \sum_{r=0}^{k-1} q_i^{\text{out}}(r). \quad (9)$$

Equation (9) considers the expected flow in DQ_i as the difference between: (i) the sum of all of the expected inflows into link i from time 0 to time $k - k^{\text{fwd}} - 1$ (i.e., omitting the flows that have still not arrived to the downstream end of the link) and (ii) the sum of all expected outflows out of link i (i.e., outflow from time 0 to time $k - 1$).

Second, we approximate $DQ_i + \sum_{\forall n \in N} UQ_n$ as a sum of independent Poisson processes. Hence, the conditional variate $\{DQ_i, UQ_n, \forall n \in N\}$ given $\{DQ_i + \sum_{\forall n \in N} UQ_n = \sum_{\forall n \in N} \ell_n\}$ follows a multinomial distribution with parameters $(\sum_{\forall n \in N} \ell_n; q^{DQ_i}/q, q^{UQ_n}/q \forall n \in N)$ (cf., for instance, Section 2.12.4 of Larson and Odoni (1981)). This leads to:

$$P \left(DQ_i = 0, UQ_n = \ell_n \forall n \in N \mid DQ_i + \sum_{\forall n \in N} UQ_n = \sum_{\forall n \in N} \ell_n \right) = \frac{(\sum_{\forall n \in N} \ell_n)!}{\prod_{n \in N} \ell_n!} \prod_{n \in N} \left(\frac{q^{UQ_n}}{q} \right)^{\ell_n}. \quad (10)$$

Note that although we ignore the temporal dependencies among the queues, the multinomial distribution parameters $(q^{DQ_i}/q$ and $q^{UQ_n}/q)$ are highly temporally dependent. With this same technique, we approximate each of the joint probabilities that appear in Equation (4).

2.2.2 Link model arrival and effective service rates

We now present how we use the expected flow between links (Equation (3)) to approximate the arrival rates and the effective service rates of a link.

Consider a node with an upstream link i . The expected outflow rate from link i is given by:

$$q_i^{out}(k) = \mu_i \left(1 - \sum_{j \in N} p_{ij} \right) P(DQ_i(k) > 0) + \sum_{j \in N} q_{i \rightarrow j}^{out}(k) \quad (11)$$

$$= \mu_i \left(1 - \sum_{j \in N} p_{ij} \right) P(DQ_i(k) > 0) + \left(\sum_{j \in N} p_{ij} \right) \mu_i P(DQ_i(k) > 0, UQ_n(k) < \ell_n \ \forall n \in N). \quad (12)$$

Equation (11) states that the expected outflow rate from link i is the summation of the expected flow rate that leaves the network through link i and the expected outflow from link i to all its downstream links j . Equation (12) is obtained by inserting the expression for $q_{i \rightarrow j}^{out}(k)$ of Equation (3).

Additionally, let $\hat{\mu}_i(k)$ denote the effective service rate of link i at time step k . The effective service rate, $\hat{\mu}_i$, differs from the service rate, μ_i , in that the former accounts for the impact of downstream spillbacks on the departure rate of link i , while the latter is an exogenous parameter that assumes the link is isolated and represents its downstream flow capacity.

By definition, the expected outflow and the effective service rate are related as follows:

$$q_i^{out}(k) = \hat{\mu}_i(k) P(DQ_i(k) > 0). \quad (13)$$

We can combine Equations (12) and (13) to obtain an expression for the effective service rate:

$$\hat{\mu}_i(k) = \frac{q_i^{out}(k)}{P(DQ_i(k) > 0)} = \mu_i \left[\left(1 - \sum_{j \in N} p_{ij} \right) + \left(\sum_{j \in N} p_{ij} \right) P(UQ_n(k) < \ell_n \ \forall n \in N \mid DQ_i(k) > 0) \right]. \quad (14)$$

Let us now describe how the expected flow between links is used to approximate the arrival rate of a link. Consider a node with downstream link j . The expected inflow rate to link j is given by:

$$q_j^{in}(k) = \gamma_j P(UQ_j(k) < \ell_j) + \sum_{i \in M} q_{i \rightarrow j}^{out}(k) \quad (15)$$

$$= \gamma_j P(UQ_j(k) < \ell_j) + \sum_{i \in M} p_{ij} \mu_i P(DQ_i(k) > 0, UQ_n(k) < \ell_n \ \forall n \in N) \quad (16)$$

where γ_j is the exogenous arrival rate to link j (i.e., it represents the rate with which trips start at link j), Equation (15) states that the expected inflow to link j is the summation of the expected flow entering the network through link j and the expected flow from all upstream links i to link j .

By definition, the expected inflow rate and the arrival rate, $\lambda_j(k)$, are related as follows:

$$q_j^{in}(k) = \lambda_j(k)P(UQ_j(k) < \ell_j). \quad (17)$$

We combine Equations (16) and (17) to obtain an expression for the arrival rate of link i at time step k :

$$\lambda_j(k) = \frac{q_j^{in}(k)}{P(UQ_j(k) < \ell_j)} = \gamma_i + \sum_{i \in M} p_{ij} \mu_i P(DQ_i(k) > 0, UQ_n(k) < \ell_n \forall n \neq j, n \in N \mid UQ_j(k) < \ell_j) \quad (18)$$

2.2.3 Algorithm

Algorithm 1 summarizes the numerical evaluation of the proposed network model for all links i in the set of links \mathcal{L} . The state distribution of link i is obtained by evaluating the mixture model of Lu and Osorio (2018) as defined in Equations (1) and (2). Notice that steps 7(a) and 7(b) in the algorithm can be run simultaneously to further enhance the runtime. Additionally, for both steps 7(a) and 7(b) the calculations for each link can be done in parallel (i.e., given their boundary conditions, links are updated independently).

3 Model validation

In this section, we validate the proposed network model formulation. We consider the following network topologies: a tandem (i.e., series) two link network (Section 3.1), a three link merge network (Section 3.2), a three link diverge network (Section 3.3) and a network with 8 links with intricate traffic dynamics (Section 3.4). The latter is the same network at that considered in Section 3 of Flötteröd and Osorio (2014). We carry out experiments with time-varying demand and varying levels of congestion.

The outputs of the analytical model are compared to estimates obtained from a discrete-event simulator of the stochastic link transmission model. This simulator has been used for validation in Osorio and Flötteröd (2015). The simulator samples individual vehicles each with exact forward and backward lags, and it satisfies FIFO. For each experiment, the simulated estimates are obtained from 10^6 simulation replications. Estimates of 95% confidence intervals were calculated, yet were barely visible. Hence, they are not displayed in the figures.

For all networks, each link consists of a single lane. The lane parameters are common to all experiments, and are displayed in Table 1. The link lengths are fixed at 50m (resp. space capacity $\ell = 10$, forward lags $k^{fwd}\delta = 5$ sec, and backward lags $k^{bwd}\delta = 10$ sec). Each experiment starts with an empty network and runs for 600 seconds.

Algorithm 1 Network model algorithm

1. set values for the exogenous parameters $\hat{\rho}_i, v_i, w_i, \ell_i$ and δ
 2. compute $k_i^{fwd} = \lceil \frac{\ell_i}{\hat{\rho}_i v_i \delta} \rceil$ and $k_i^{fwd} = \lceil \frac{\ell_i}{\hat{\rho}_i |w_i| \delta} \rceil$
 3. compute \hat{w}_i according to Eq. (37) of Lu and Osorio (2018)
 4. set initial conditions: $q_i^{in}(0), q_i^{out}(0), P^{UQ}(UQ_i(0)), P^{DQ}(DQ_i(0)), q^{UQ_i}(0), q^{LLO_i}(0), q^{LLI_i}(0), q^{DQ_i}(0), \lambda_i(0)$ and $\hat{\mu}_i(0)$.
 5. set $q_i^{in}(r) = 0$ and $q_i^{out}(r) = 0$ for $r < 0$
 6. repeat the following for time intervals $k = 1, 2, \dots$
 - (a) for all links i , evaluate the univariate UQ model (i.e., run Algorithm 1 of Lu and Osorio (2018)) with initial conditions $P^{UQ}(UQ_i(k-1)), \hat{\mu}_i(k-1)$ and $\lambda_i(k-1)$, this yields $P^{UQ}(UQ_i(k)), P^{UQ}(DQ_i(k))$
 - (b) for all links i , evaluate the univariate DQ model (i.e., run Algorithm 2 of Lu and Osorio (2018)) with initial conditions $P^{DQ}(DQ_i(k-1)), \hat{\mu}_i(k-1)$ and $\lambda_i(k-1)$, this yields $P^{DQ}(DQ_i(k)), P^{DQ}(UQ_i(k))$
 - (c) calculate $P(DQ_i(k) > 0, UQ_n(k) < \ell_n \forall n \in N)$ according to Eq. (4)
 - (d) calculate $q_{i \rightarrow j}^{out}(k)$ according to Eq. (3)
 - (e) calculate $q_i^{in}(k), q_i^{out}(k)$ according to Eq. (15) and (11), respectively.
 - (f) calculate $\hat{\mu}_i(k)$ and $\lambda_i(k)$ according to Eq. (14) and (18), respectively.
-

3.1 Two link tandem network

The topology of the network with two links in tandem is displayed in Figure 1, where vertices represent intersections and edges represent links. Both links are directed (as indicated by arrows). Link 1 is the source link with exogenous arrival rate λ_1 and exogenous service rate μ_1 . Link 2 is the terminal link with endogenous arrival rate λ_2 and exogenous service rate μ_2 . All trips start at link 1 and end at link 2, i.e., no trips start at link 2.

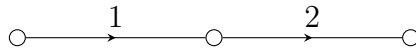


Figure 1: Network of two tandem links

We conduct 4 experiments with time-varying demand and different service rates. The concrete parameters used are shown in Table 2. For each experiment, the arrival rate is 0.15 veh/sec during time $[0,200]$ seconds, 0.05 veh/sec during time $[200,400]$ seconds and 0.25 veh/sec during time $[400,600]$ seconds.

Figure 2 displays $E[UQ(T)]$ and $E[DQ(T)]$ as a function of time T for experiments 1 through

Table 1: Link Parameters

Parameter	Value
v	0.01 km/sec
w	-0.005 km/sec
$\hat{\rho}$	200 veh/km
\hat{q}	2400 veh/h = 0.67 veh/sec
δ	0.1 sec
L (ℓ, k^{fwd}, k^{bwd})	50 m (10, 50, 100)

Table 2: Experimental design for the two link tandem network

Experiment	$\lambda_1(k)$	μ_1	μ_2
1	0.15 \rightarrow 0.05 \rightarrow 0.25	0.4	0.4
2	0.15 \rightarrow 0.05 \rightarrow 0.25	0.4	0.2
3	0.15 \rightarrow 0.05 \rightarrow 0.25	0.2	0.2
4	0.15 \rightarrow 0.05 \rightarrow 0.25	0.2	0.4

4. Figure 2(a) shows the results for experiment 1. The left (resp. right) graph considers link 1 (resp. 2). Each graph displays $E[UQ(T)]$ (solid lines) and $E[DQ(T)]$ (dashed lines). Black lines represent simulated results and red lines represent analytical results. The sharp decrease in expectation from time $T = 200$ to $T = 400$ seconds and the sharp increase in expectation after time $T = 400$ are both well approximated by the proposed model. The proposed model estimates the expectation accurately for the first 400 seconds, but slightly overestimates it for the last 200 seconds. Figures 2(b), 2(c) and 2(d) show the results for experiments 2, 3 and 4, respectively. The changes in expectation caused by the time-varying demand are well approximated by the proposed model. For instance, during the last 200 seconds of experiment 2, the sharp increase in demand causes spillback on link 2. Both the occurrence of spillback on link 2 and its impact on link 1 are captured by the proposed model. Overall, the approximation of the proposed model is accurate.

3.2 Three link merge network

The topology of the three link merge networks is shown in Figure 3. Vehicles enter the network by joining link 1 or 2, and they leave the network through link 3. The service rates μ_i for link i ($i = 1, 2, 3$) are exogenous, and the arrival rates λ_i to links 1 and 2 ($i \in \{1, 2\}$) are exogenous, whereas λ_3 is endogenous. We conduct 2 experiments with time-varying demand for link 1 and constant demand for link 2. The experimental design is detailed in Table 3. For each experiment, the arrival rate is 0.15 veh/sec during time $[0, 200]$ seconds, 0.25 veh/sec during time $[200, 400]$ seconds and 0.05 veh/sec during time $[400, 600]$ seconds.

For experiment 5, the congestion level of link 1 is expected to increase and then decrease, while link 2 is expected to be uncongested. During the first 400 seconds a spillback from link 3 to links 1 and 2 is expected. For experiment 6, link 1 is expected to be congested for the first 400 seconds and uncongested thereafter. Link 2 is expected to be congested, and link 3 is expected

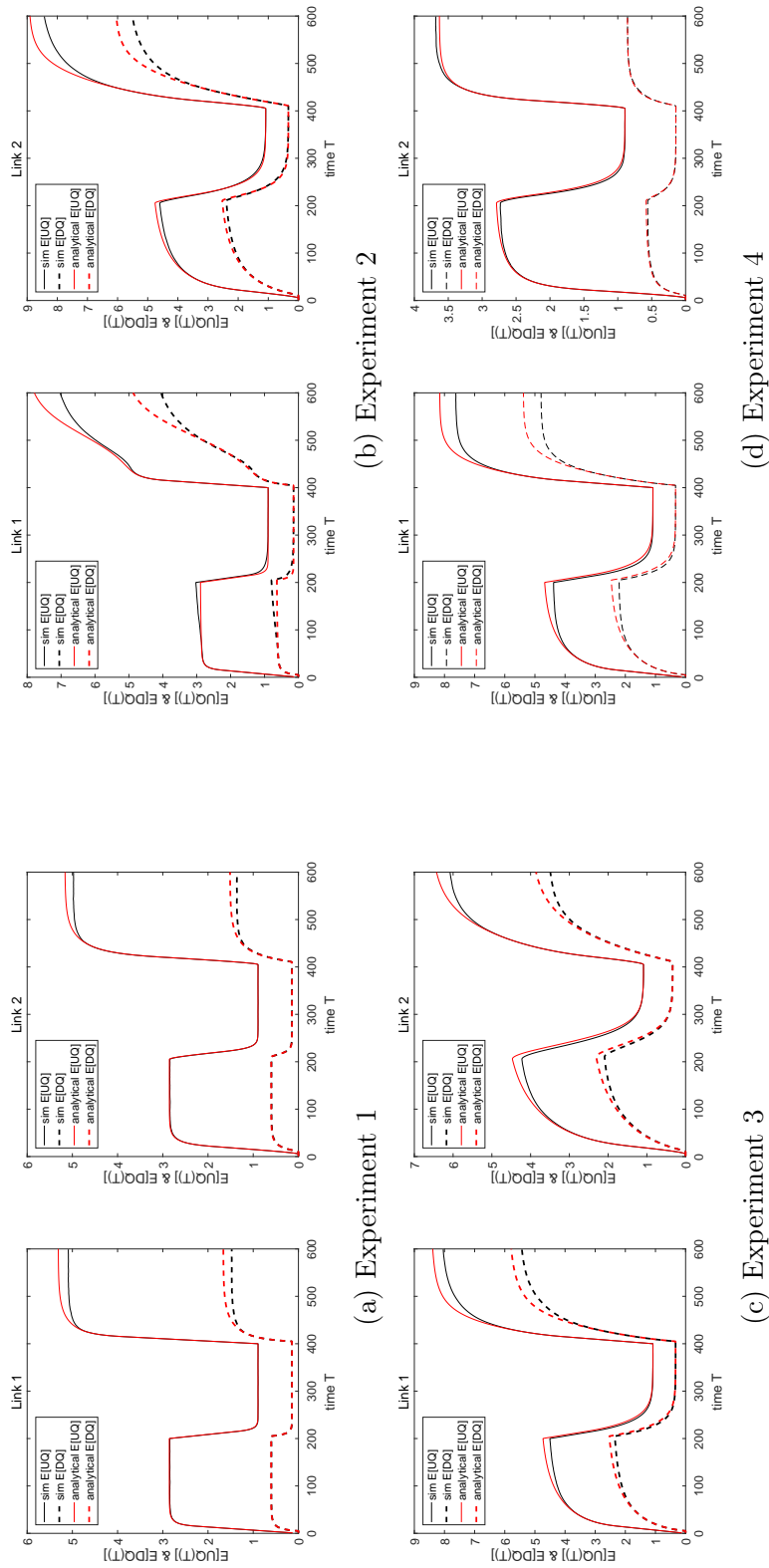


Figure 2: $E[UQ(T)]$ and $E[DQ(T)]$

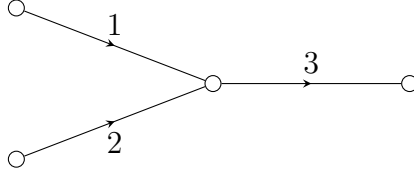


Figure 3: Merge network of three links

Table 3: Experimental design for merge network

Experiment	λ_1	μ_1	λ_2	μ_2	μ_3
5	0.15 \rightarrow 0.25 \rightarrow 0.05	0.4	0.05	0.2	0.2
6	0.15 \rightarrow 0.25 \rightarrow 0.05	0.2	0.15	0.2	0.6

to be uncongested all the time. Figure 4(a) (resp. Fig. 4(b)) displays $E[UQ(T)]$ and $E[DQ(T)]$ as a function of time T for experiment 5 (resp. experiment 6).

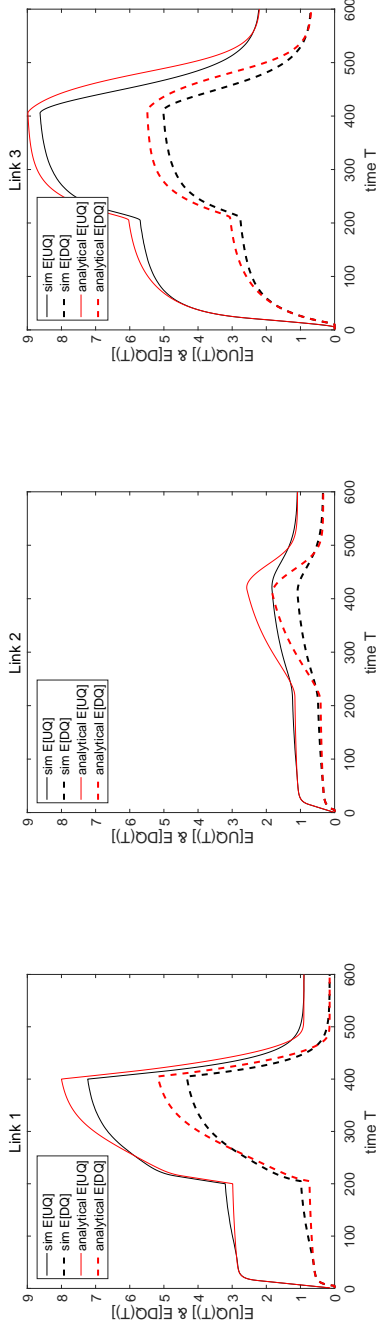
The line styles and colors are the same as for the previous figures. The plots in columns 1, 2, and 3 display, respectively, the results for links 1, 2 and 3. For link 1, there is, as expected, an increase in expectation during time [200, 400] seconds, which is caused by both the increase in demand and the occurrence of spillback from link 3. Then, there is a sharp decrease after time $T = 400$ seconds caused by the decrease in demand and the spillback dissipation.

For link 2 (middle plot), there is an increase in expectation during time [200, 400] seconds. This increase is purely caused by the spillback from link 3. For link 3, there is an increase in expectation during time [200, 400] seconds and a decrease after time $T = 400$ seconds caused by the changes in demand of link 1. During time [200, 400] seconds, $E[UQ(T)]$ almost reaches the space capacity and causes a significant spillback effect from link 3 to links 1 and 2. For all three plots of Figure 4(a), the proposed analytical model yields approximations which accurately capture the trends of the simulated estimates. However, the proposed model overestimates the spillback of link 3, and its effect on links 1 and 2.

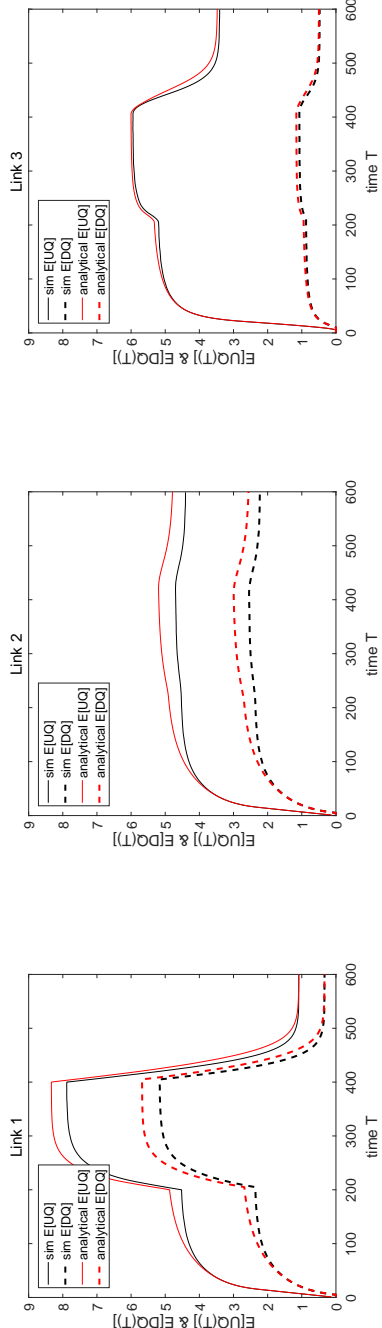
Figure 4(b) displays the results of experiment 6. It has the same structure as Figure 4(a). The increase and decrease in demand of link 1 causes the increase and decrease in expectation for both links 1 and 3. For link 2 with constant demand, there is a subtle increase and decrease in expectation. Even this subtle change is captured by the proposed model. Overall, the proposed model captures the temporal variations of these performance metrics accurately.

3.3 Three link diverge network

The topology of the three link diverge network is shown in Figure 5. Vehicles enter the network by joining link 1 at a rate λ_1 . From link 1, they continue to either link 2 with turning probability p_{12} or to link 3 with probability p_{13} (i.e., $p_{13} = 1 - p_{12}$). The two experiments that we conduct consider time-varying demand for link 1 and different turning probabilities. The experimental design is presented in Table 4. For each experiment, the arrival rate is 0.2 veh/sec during time [0,200] seconds, 0.4 veh/sec during time [200,400] seconds and 0.1 veh/sec during time [400,600] seconds.



(a) Experiment 5



(b) Experiment 6

Figure 4: $E[UQ(T)]$ and $E[DQ(T)]$

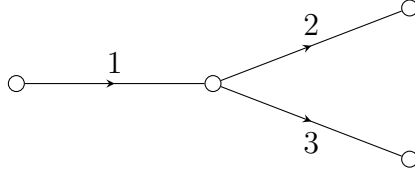


Figure 5: Diverge network of three links

Table 4: Experimental design for diverge network

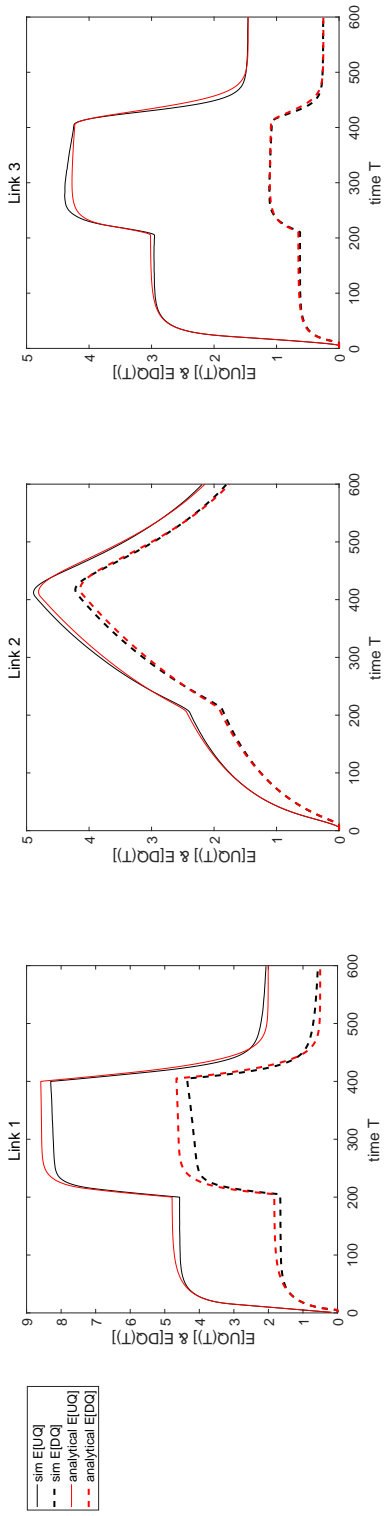
Experiment	λ_1	μ_1	μ_2	μ_3	p_{12}
7	0.2 \rightarrow 0.4 \rightarrow 0.1	0.3	0.05	0.4	0.2
8	0.2 \rightarrow 0.4 \rightarrow 0.1	0.6	0.4	0.4	0.5

For both experiments 7 and 8, the congestion level of all links is expected to increase and then decrease over time. For experiment 7, the congestion levels of downstream links 2 and 3 will differ. For experiment 8, both downstream links have identical configuration, and the vehicles have equal probability of choosing either link, hence we expect the congestion levels of links 2 and 3 to be identical.

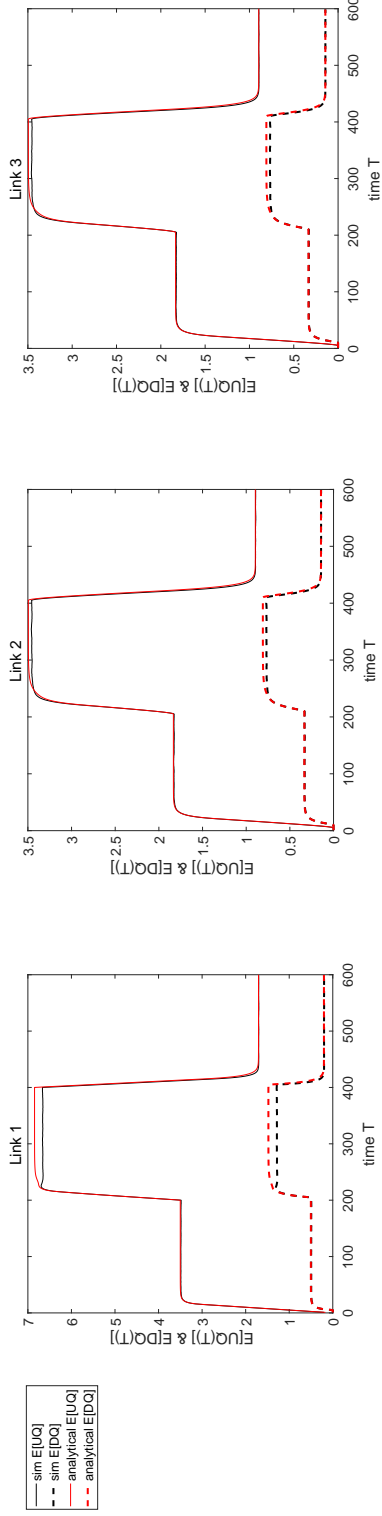
Figure 6(a) shows the results for experiment 7. The graphs from left to right display $E[UQ(T)]$ and $E[DQ(T)]$ for links 1, 2, and 3, respectively. As a first impression, the deviations between analytical and simulated expectations are small. The shapes of expectation curves for links 2 and 3 are different. The sharp increase in expectation during the second 200 seconds and the sharp decrease in expectation after 400 seconds for all three links are well approximated by the proposed model. Figure 6(b) shows the results for experiment 8. The proposed model yields identical expectation curves for links 2 and 3, as expected. The analytical approximate expectations match the simulated estimates. The proposed model accurately captures the temporal variations, in both shape and magnitude, of these performance metrics.

3.4 Eight link network

Finally, we consider an eight link network with intricate traffic dynamics. The network topology is given in Figure 7. This network configuration is the same as in Flötteröd and Osorio (2014). Vehicles enter the network by joining links 1 or 2. They can leave the network through links 3 and 4. Upon entrance to link 1 (resp. 2), vehicles can either go straight to link 6 (resp. 8) and leave the network through link 4 (resp. 3) or initiate a U-turn to link 5 (resp. 7) and leave the network through link 3 (resp. 4). The concrete parameters used for this network are as follows. Vehicles can enter the network through links 1 or 2. For link 1, vehicles enter at a rate of 0.1 veh/sec during [0,200] seconds, 0.2 veh/sec during [200, 400] seconds and 0.15 veh/sec during [400,600] seconds. For link 2, vehicles enter at a rate of 0.1 veh/sec during [0,200] seconds, 0.15 veh/sec during [200, 400] seconds and 0.2 veh/sec during [400,600] seconds. They continue straight with probability $p_{16} = p_{28} = 2/3$ and perform a U-turn with probability $p_{15} = p_{27} = 1/3$. The service rates for link 1 and 2 are $\mu_1 = \mu_2 = 0.25$ veh/sec and the service rates for the links within the network are $\mu_5 = \mu_6 = \mu_7 = \mu_8 = 0.4$ veh/sec, which is on



(a) Experiment 7



(b) Experiment 8

Figure 6: $E[UQ(T)]$ and $E[DQ(T)]$

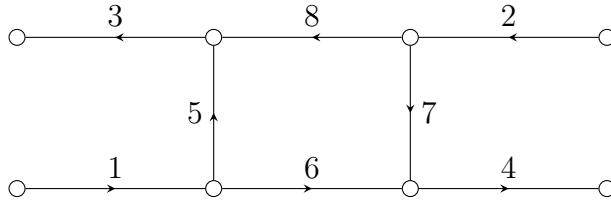


Figure 7: Toy network of eight links

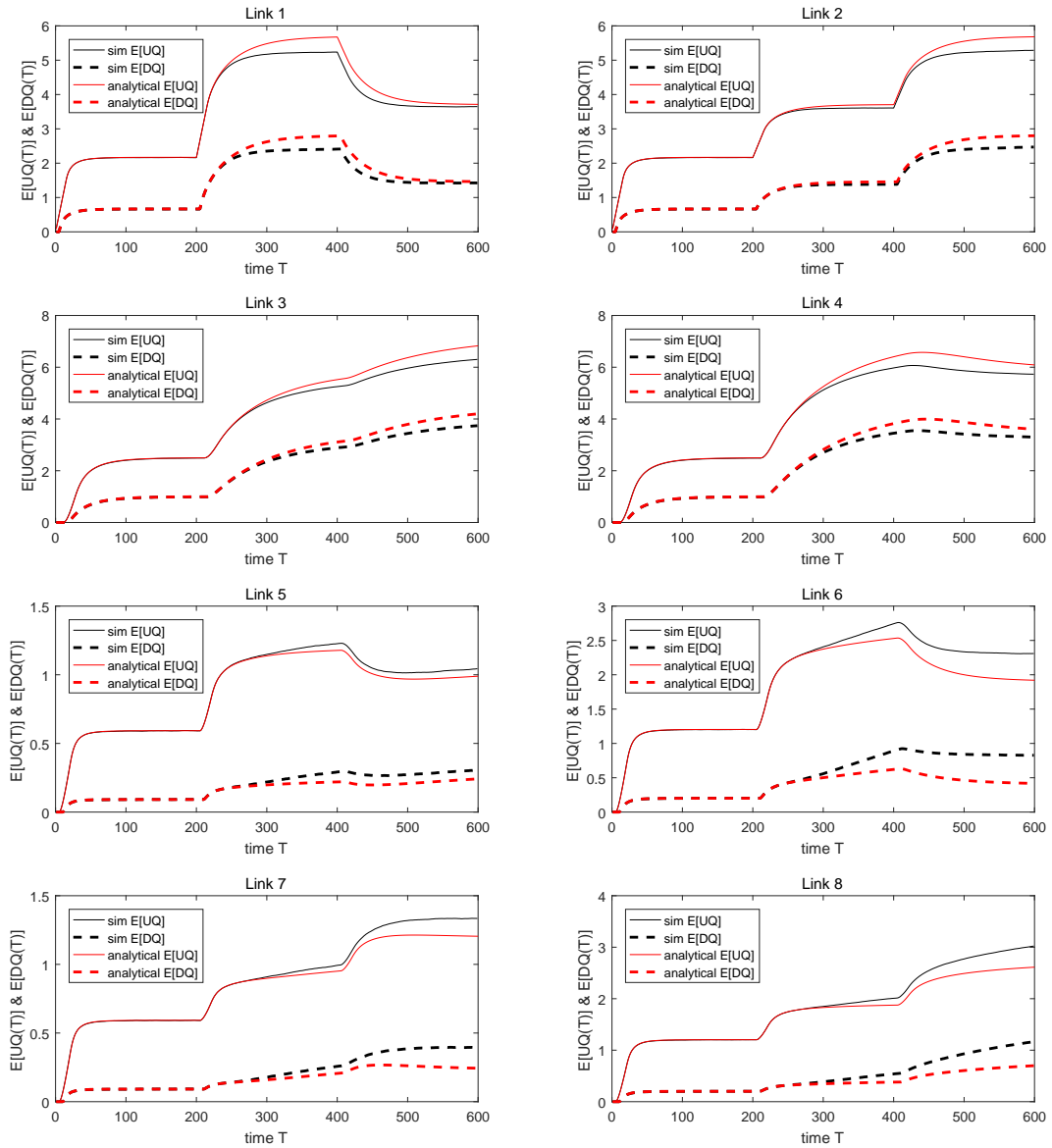


Figure 8: $E[UQ(T)]$ and $E[DQ(T)]$ for the experiment on toy network

average sufficient to serve the demand. The service rates for exit links 3 and 4 are lower at $\mu_3 = \mu_4 = 0.2$ veh/sec.

The difference in time-varying demands at the two source links 1 and 2 leads to intricate traffic patterns. The congestion patterns that we expect to observe based on this experimental design are as follows. Link 1 experiences step-changes from uncongested to congested, and then again to uncongested conditions. Link 2, on the other hand, experiences step-changes steadily from uncongested to congested conditions. For the first 200 seconds, the exit link 3 (resp. 4) is uncongested, hence the congestion level of its upstream links 5 and 8 (resp. 6 and 7) are determined by the outflow from their respective upstream links 1 (resp. 2). After 200 seconds, travel demand increases. Thus, the occurrence of spillback on the exit link 3 (resp. 4) increases, this impacts the congestion levels of its upstream links 5 and 8 (resp. 6 and 7).

Each plot of Figure 8 shows the evolution of $E[UQ(T)]$ and $E[DQ(T)]$ for one of the eight links in the network. The line styles and colors are the same as for the previous figures. The temporal variations of the analytical approximations mimic well the simulated variations. However, it tends to underestimate the congestion levels of links 6 and 8.

In summary, the proposed model captures the temporal evolution in expectations for this network with intricate traffic patterns. Additionally, it does so with a significant gain in computational efficiency. For instance, since each link of this network has a space capacity of 10, the state space of the joint network distribution has dimension 11^8 . The proposed model overcomes the need to model the entire joint distribution. Instead, the memory required for the proposed model is $2 \times 11 \times 8 = 176$ numbers. This represents a significant gain in computational efficiency, and enables its use for large-scale network analysis and optimization.

4 Case study

In this section, the proposed network model is used to address an optimization problem. The purpose of this section is to investigate the added value of the proposed network model, and more specifically of the node model, for traffic control. We consider a fixed-time signal control problem for the network shown in Figure 9. The representation of the road network as a single-lane network is presented in Figure 10. Section 4.1 formulates the problem and describes the case study. Section 4.2 presents the numerical results.

We address the problem with our proposed model. We also solve it with the link model of Lu and Osorio (2018) (this is the mixture model described in Section 2.1) and with an exogenous node model (described in Section 4.1 of Lu and Osorio (2018)). Hereafter, we call the latter approach the marginal network model. In the marginal network model, the total demand to each link is exogenous. Hence, each link can be modeled independently. That is, this marginal model accounts for the within-link temporal variations of congestion, but does not capture any between-link (i.e., across-node) interactions. In other words, both models (proposed and marginal) consider the same link models. The proposed model has an endogenous node model (formulated in Section 2.2) which captures the between-link interactions, while the marginal model omits between-link interactions. We use both models to address the optimiza-

tion problem. We then compare their results. This comparison will indicate the added value of accounting for between-link interactions in traffic control.

Additionally, the deterministic intelligent link transmission model (ILTM) (Himpe et al., 2016), which is a complete network loading model that embeds the well-established node model of Tampère et al. (2011a), is applied to address the same problem. The comparison between the results between ILTM and the proposed model will indicate the added value of accounting for stochasticity in traffic control.

4.1 Network configuration and problem formulation

We consider a small synthetic network, which is displayed in Figure 9. The network consists of 20 single-lane roads and 4 intersections, each with 2 endogenous signal phases. The circles in Figure 9 are where the vehicles can enter and leave the network. We consider a fixed-time signal control problem. We refer the reader to Appendix A of Osorio (2010) for a review of traffic signal control terminology and formulations. A fixed-time signal plan, also called time-of-day or pre-timed plan, is an off-line pre-determined plan. It uses historical traffic data to derive a fixed periodical plan during a specific time of day (e.g., evening peak). Fixed-time signal plans are commonly used for networks with sparse or unreliable real-time data, they are also used by major cities, such as New York City Osorio et al. (2016), with high and uniformly distributed congestion levels.

We consider a fixed-time signal control problem for a 30 min period. The signal plans of the 4 intersections are jointly determined. The decision variables are the green splits of the phases of the different intersections. All other traditional control variables (e.g., cycle times, offsets, stage structure) are assumed fixed. There are 2 endogenous signal phases per intersection. Hence, the dimension of the decision variable vector is 8.

To formulate the signal control problem, we introduce the following notation:

b_d	ratio of available cycle time to total cycle time for intersection d ;
x	vector of green splits;
$x(j)$	green split of signal phase j ;
x_{LB}	vector of lower bounds for green splits;
\mathcal{D}	set of intersection indices;
$\mathcal{P}_D(d)$	set of endogenous signal phase indices of intersection d ;
\mathcal{L}	set of all links;
\tilde{T}	the length of the time interval of interest [in min];
$ \mathcal{L} $	the number of links, i.e., cardinality of \mathcal{L} .

The problem is formulated as follows:

$$\min_x f(x) = \frac{1}{\tilde{T}|\mathcal{L}|} \sum_{i \in \mathcal{L}} \sum_{\hat{t}=1}^{\tilde{T}} E[DAQ_i(\hat{t}; x)] \quad (19)$$

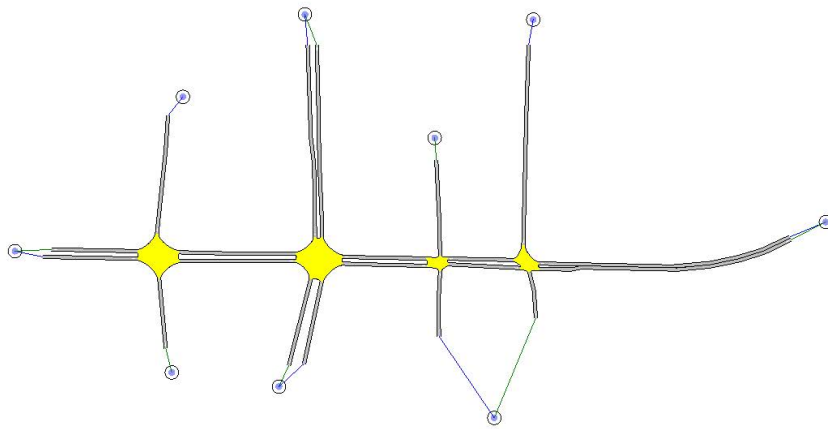


Figure 9: Network topology

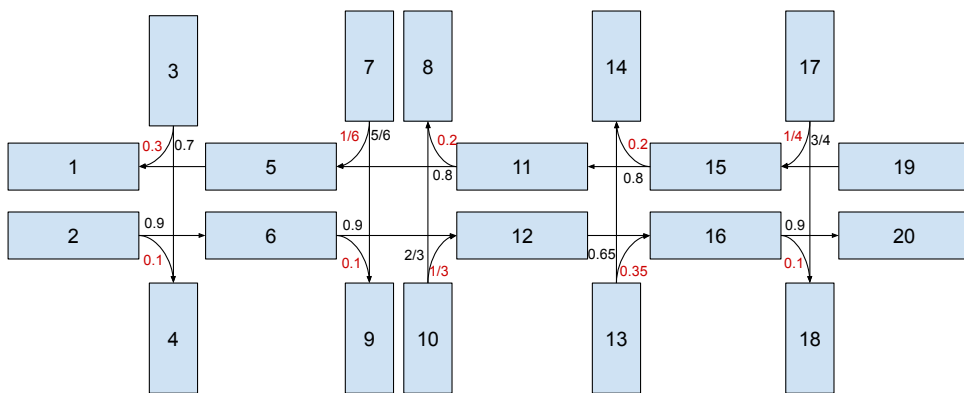


Figure 10: Network model

subject to

$$\sum_{j \in \mathcal{P}_D(d)} x(j) = b_d, \quad \forall d \in \mathcal{D} \quad (20)$$

$$x \geq x_{LB}. \quad (21)$$

The decision vector, x , denotes the green splits of the signal controlled links. Constraint (20) ensures that for each intersection, the sum of green splits equals the available cycle time. Constraint (21) ensures lower bounds for the green splits. The objective function represents the average, over time and over links, of the expectation of DQ . $E[DQ_i(\hat{t}; x)]$ denotes the expectation of DQ of link i at integer time \hat{t} (in minutes) under signal plan x . It is calculated by evaluating either the proposed network model or the marginal link model.

For the deterministic ILTM, the objective function is the average, over time and over the network lanes, number of vehicles on the link, i.e.,

$$f(x) = \frac{1}{\bar{T}|\mathcal{L}|} \sum_{i \in \mathcal{L}} \sum_{\hat{t}=1}^{\bar{T}} (c_i^{up}(\hat{t}; x) - c_i^{down}(\hat{t}; x)). \quad (22)$$

where $c_i^{up}(\hat{t}; x)$ (resp. $c_i^{down}(\hat{t}; x)$) is the cumulative number of vehicles that cross the upstream (resp. downstream) end of link i up until time \hat{t} under signal plan x , which is the output metric produced by the deterministic ILTM model.

Note that the decision variables (i.e., the green splits) are related to the link parameters as follows. Given a signal plan, the service rate, μ_i , of signalized link i is determined by the following equation.

$$\mu_i - \sum_{j \in \mathcal{P}_I(i)} x(j)s = e_i s \quad (23)$$

where s represents the saturation flow, e_i represents the ratio of fixed green time to cycle time and $\mathcal{P}_I(i)$ represents the set of endogenous signal phases of link i . The deterministic ILTM also considers an average outflow capacity as suggested by the developers. This is because the explicit implementation of traffic cycles comes at a cost of more memory use (which can be prohibitive in Matlab) and higher computation times.

Table 5 displays the values of the main exogenous model parameters. Note that there are two sets of demand scenarios in Section 4 of Osorio and Yamani (2017), high demand and medium demand, we are going to carry out the optimization for both demand scenarios. The optimization problems are solved using the *Active-set* algorithm of the *fmincon* routine of MATLAB (2016).

4.2 Numerical analysis

To initialize the algorithm, we randomly and uniformly draw a point from the feasible space (Equations (20)-(21)). We use the code of Stafford (2006) to perform this uniform sampling.

Table 5: Parameters for the case study

Parameter	Value
\tilde{T}	15 min
$ \mathcal{L} $	20 links
δ	0.1 sec
x_{LB}	4 sec
v	50 km/h
w	-15 km/h
$\hat{\rho}$	200 veh/km
s	1800 veh/h
μ	varies by signal plans
ℓ, γ	exogenous values from section 4 of Osorio and Yamani (2017)
p_{ij}	turning fractions is shown in Figure 10
k^{fwd}	$k^{fwd} = \lceil \frac{\ell}{\hat{\rho}v} \rceil$
k^{bwd}	$k^{bwd} = \lceil \frac{\ell}{\hat{\rho} w } \rceil$

We initialize the proposed network model, the marginal model and the ILTM with the same random initial point. We then solve Problem (19)-(21) with each of the two models. Each model yields an optimal signal plan. To evaluate the performance of a given signal plan, we use a microscopic traffic simulation model implemented with the Aimsun simulator (TSS, 2014). For a given signal plan, we embed it within the simulator and run 50 simulation replications. Each simulation replication simulate a 30 min period. Each replication yields one observation of the main performance measures: average link queue-length and average trip travel time. We then compare the cumulative distribution functions (cdf's) obtained from the 50 replications of these performance measures.

Figures 11(a) and 11(b) consider the average link queue-length for high and medium demand scenarios, respectively. For each demand scenario, it displays four cdf curves: the signal plan derived by the proposed network model is displayed with a solid curve, that of the marginal model is displayed with a thick dot-dashed curve, that of the ILTM is displayed with crossed solid curve and that of the initial plan is displayed with a dashed curve. The average link queue-length is an average obtained over time and over all links of the network. The x -axis displays the average link queue-length in vehicle. For given x value, the y -axis displays the proportion of simulation replications (out of 50) that have average queue-lengths smaller than x . Therefore, the more a cdf curve is shifted to the left, the better the performance of the corresponding signal plan.

Figure 11(a) indicates that the proposed network, the marginal models and ILTM all yield plans with improved performance compared to the initial plan for high demand scenario. Additionally, the cdf curve of the derived signal plan from the proposed model is to the left of both the derived signal plans from ILTM and the marginal model. This indicates the signal plan derived by the proposed network model outperforms that derived by ILTM and by the marginal model. The signal plan of the proposed network model yields a 25% improvement in average link queue-length compared to the signal plan of the marginal model (2.31 versus 3.06) and a 14%

improvement compared to ILTM (2.31 versus 2.69).

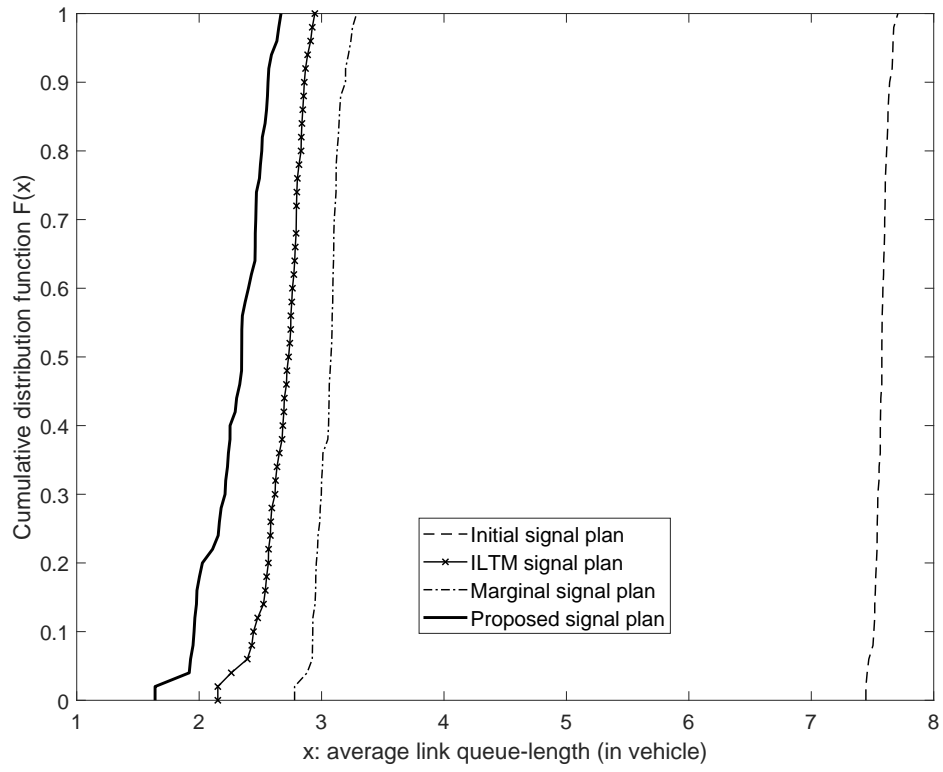
For medium demand scenarios, ILTM does not detect objective function improvement direction at the initial point and hence the optimization stopped with the initial point randomly generated. Therefore, in Figure 11(b), the curve of the ILTM completely overlaps with that of the initial signal plan. This is because ILTM calculates the deterministic average inflow and outflow capacity of the link over time and hence the model is not sensitive to the change of outflow capacity as long as it is large enough to allow all inflow to pass through. On the other hand, the stochastic models are sensitive to changes in outflow capacity (i.e., μ). The cdf curves of the derived signal plan from both the proposed and the marginal model are to the left of the derived signal plans from ILTM. This indicates the signal plans derived by the proposed and marginal model outperform that derived by ILTM. Additionally, the proposed model outperforms the marginal model and yields a 55% improvement in average link queue-length (0.97 versus 2.13).

Figures 12(a) and 12(b) compare the performance of the four signal plans considering the average trip travel times (in minutes) for high and medium demand scenarios, respectively. The x -axis shows average trip travel time. the y -axis displays the proportion of simulation replications (out of 50) that have average trip travel times smaller than x . Figure 12 has similar layout as Figure 11. The same conclusions as for Figure 11 hold. The proposed model yields a signal plan that outperforms the initial plan, the ILTM and the plan derived by the marginal model in both high and medium demand scenarios. The signal plan of the proposed network model yields an 35% improvement in average trip travel time compared to the signal plan of the marginal model (0.99 minutes versus 1.53 minutes) in medium demand scenario and 19% improvement in high demand scenario (1.48 minutes versus 1.82 minutes). The proposed model outperforms the deterministic ILTM in both demand scenarios.

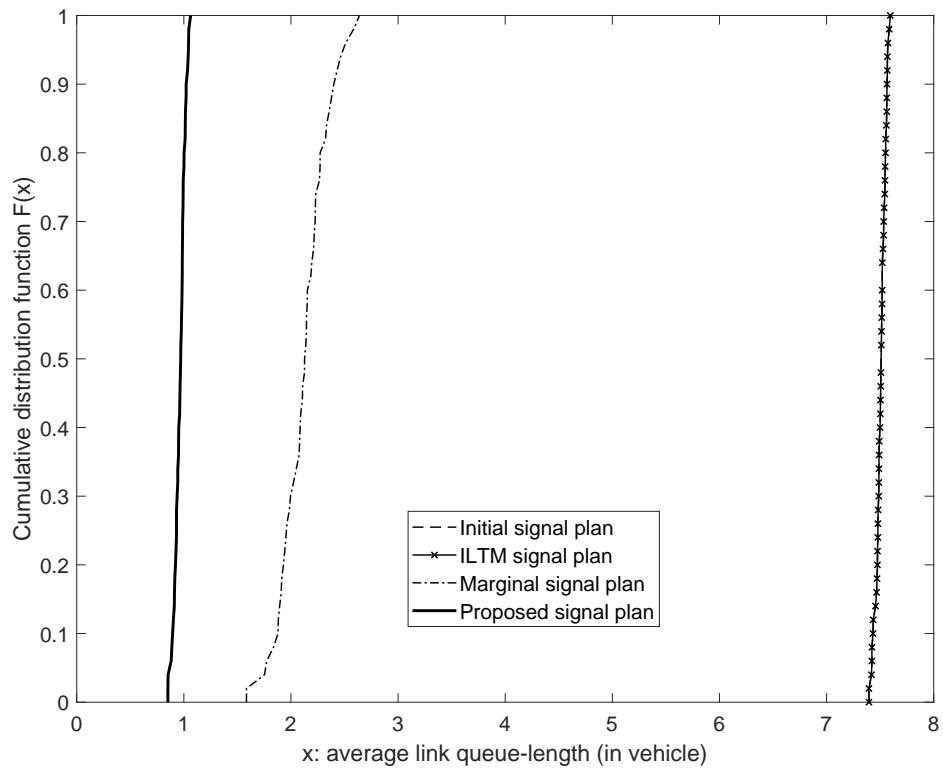
The results of this case study indicate that the coupling of the link model with the node model allows to identify signal plans with improved performance. The results indicate the ability of the proposed node model to describe the occurrence and impact of vehicular spillbacks and, more generally, the between-link interactions. Moreover, the results of this case study indicate that by considering stochasticity, the proposed model is able to identify signal plans with better and more robust performance. These results highlight the added value of accounting for these between-link interactions for traffic control and accounting for stochasticity in the network.

5 Conclusion

This paper formulates an analytical stochastic node model. It formulates a full network model by coupling the node model with the link model of Lu and Osorio (2018). The network model is scalable and tractable, since it only tracks univariate distributions. All higher-order distributions (i.e., multivariate) are approximated analytically. In particular, the node model is not based on the joint modeling of all upstream and downstream links adjacent to a node. Instead the joint probabilities are approximated from the univariate distributions of the upstream and downstream links. The node model is formulated for nodes with an arbitrary configuration, it satisfies flow conservation properties. It can also be coupled with other link models, e.g., Osorio et al. (2011); Osorio and Flötteröd (2015); Lu (2020). The proposed network model is

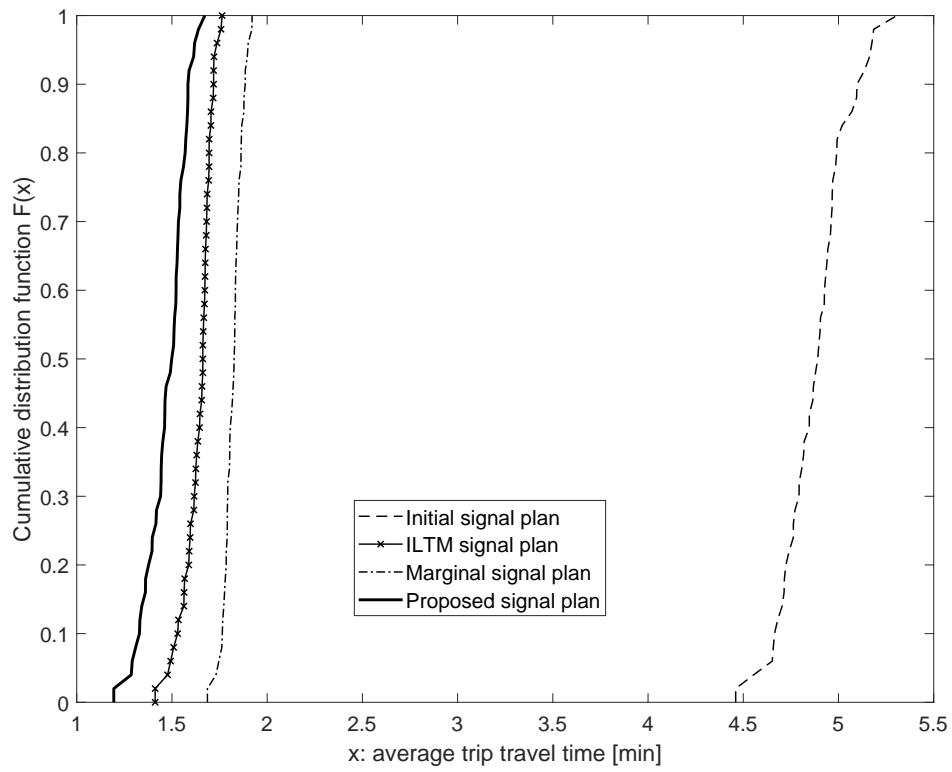


(a) High demand scenario

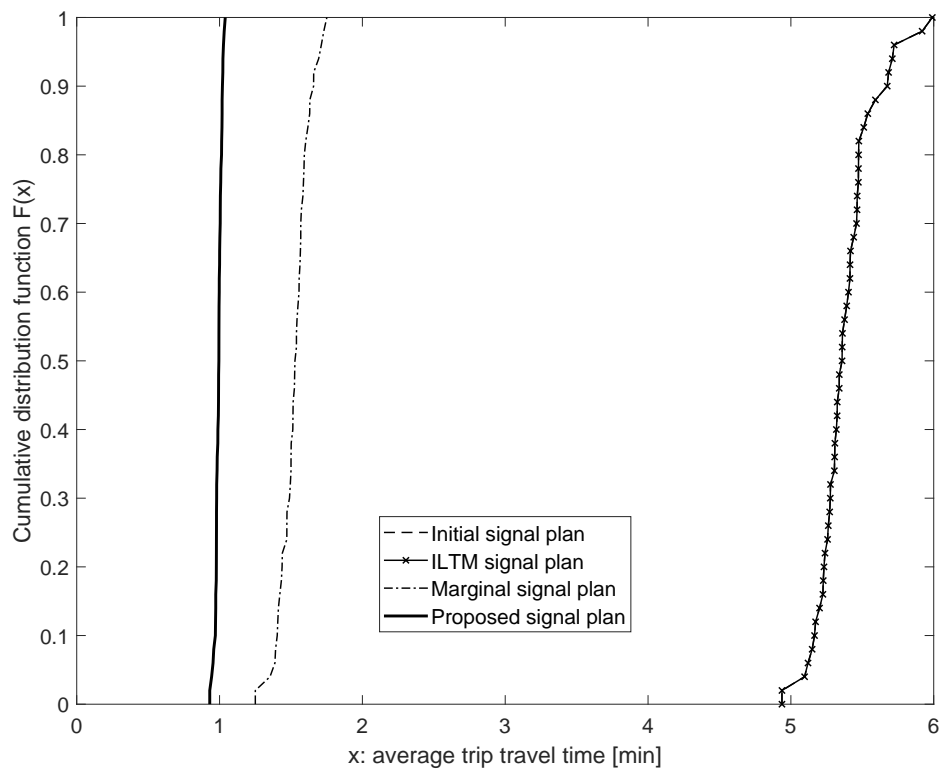


(b) Medium demand scenario

Figure 11: Cumulative distribution functions of the average, over all lanes in the network, link queue-length in vehicles.



(a) High demand scenario



(b) Medium demand scenario

Figure 12: Cumulative distribution functions of the average trip travel time in minutes.

validated versus stochastic simulation results, using a simulator of the stochastic link transmission model. We consider a set of small networks with intricate time-varying congestion patterns. The boundary conditions of every link in the network are well approximated by the proposed network model. The proposed model is used to address a signal control problem for a small network. We compare the performance of the proposed approach to that of a model with the same link model but without a node model (i.e., between-link interactions are not captured) as well as a deterministic ILTM with well-established deterministic node model. The proposed network model yields signal plans that outperform the simpler marginal model as well as the deterministic ILTM. This case study shows both the added value of accounting for the across-link dynamics for traffic management and the added value of taking stochasticity in consideration

For a network with n links, each with space capacity ℓ , a network model that tracks the entire network state space, would have a complexity of $\mathcal{O}(\ell^n)$. Instead, the complexity of the proposed network model is $\mathcal{O}(n\ell)$. Hence, the proposed approach is scalable and suitable for network analysis and optimization. Ongoing work investigates formulations to approximate the full joint network distribution. For instance, we plan to combine the proposed approach with ideas from the network decomposition method of Flötteröd and Osorio (2014). We are also investigating the use of aggregation-disaggregation techniques to approximate the full joint network distribution in a scalable and tractable way. Aggregation-disaggregation ideas address the curse of dimensionality by providing an aggregate description of network states (Osorio and Yamani, 2017; Osorio and Wang, 2017).

6 Acknowledgment

The work of J. Lu and C. Osorio are partially supported by the U.S. National Science Foundation under Grant No. 1562912. Any opinions, findings, and conclusions or recommendations expressed in this material are those of the authors and do not necessarily reflect the views of the National Science Foundation.

References

- Björklund, A., Husfeldt, T., Koivisto, M., 2009. Set partitioning via inclusion-exclusion. *SIAM Journal on Computing* 39, 546–563.
- Bliemer, M.C., 2007. Dynamic queuing and spillback in analytical multiclass dynamic network loading model. *Transportation research record* 2029, 14–21.
- Boel, R., Mihaylova, L., 2006. A compositional stochastic model for real time freeway traffic simulation. *Transportation Research Part B: Methodological* 40, 319–334.
- Comert, G., 2013. Simple analytical models for estimating the queue lengths from probe vehicles at traffic signals. *Transportation Research Part B: Methodological* 55, 59–74.

- Comert, G., 2016. Queue length estimation from probe vehicles at isolated intersections: Estimators for primary parameters. *European Journal of Operational Research* 252, 502–521.
- Comert, G., Cetin, M., 2009. Queue length estimation from probe vehicle location and the impacts of sample size. *European Journal of Operational Research* 197, 196–202.
- Comert, G., Cetin, M., 2011. Analytical evaluation of the error in queue length estimation at traffic signals from probe vehicle data. *IEEE Transactions on Intelligent Transportation Systems* 12, 563–573.
- Corthout, R., Flötteröd, G., Viti, F., Tampère, C.M., 2012. Non-unique flows in macroscopic first-order intersection models. *Transportation Research Part B: Methodological* 46, 343–359.
- Daganzo, C., 2005. A variational formulation of kinematic waves: basic theory and complex boundary conditions. *Transportation Research Part B* 39, 187–196.
- Daganzo, C.F., 1995. A finite difference approximation of the kinematic wave model of traffic flow. *Transportation Research Part B: Methodological* 29, 261–276.
- Deng, W., Lei, H., Zhou, X., 2013. Traffic state estimation and uncertainty quantification based on heterogeneous data sources: A three detector approach. *Transportation Research Part B* 57, 132 – 157.
- Flötteröd, G., Osorio, C., 2014. Analytical approximation of transient joint queue-length distribution with finite capacity markovian networks, in: *Proceedings of the International Symposium of Dynamic Traffic Assignment (DTA)*.
Available at: <http://web.mit.edu/osorioc/www/papers/floOso13Nwks.pdf> .
- Flötteröd, G., Osorio, C., 2017. Stochastic network link transmission model. *Transportation Research Part B* 102, 180–209.
- Flötteröd, G., Rohde, J., 2011. Operational macroscopic modeling of complex urban road intersections. *Transportation Research Part B: Methodological* 45, 903–922.
- Heidemann, D., 2001. A queueing theory model of nonstationary traffic flow. *Transportation Science* 35, 405–412.
- Himpe, W., Corthout, R., Tampère, M.C., 2016. An efficient iterative link transmission model. *Transportation Research Part B* 92, 170–190.
- Jabari, S.E., 2012. *A Stochastic Model of Macroscopic Traffic Flow: Theoretical Foundations*. Ph.D. thesis. University of Minnesota.
- Jabari, S.E., 2016. Node modeling for congested urban road networks. *Transportation Research Part B: Methodological* 91, 229–249.
- Jabari, S.E., Liu, H.X., 2012. A stochastic model of traffic flow: Theoretical foundations. *Transportation Research Part B: Methodological* 46, 156–174.

- Jabari, S.E., Liu, H.X., 2013. A stochastic model of traffic flow: Gaussian approximation and estimation. *Transportation Research Part B* 47, 15–41.
- Larson, R.C., Odoni, A.R., 1981. *Urban Operations Research*. Prentice-Hall, Inc., Englewood Cliffs, New Jersey, USA.
- Laval, J.A., Castrillón, F., 2015. Stochastic approximations for the macroscopic fundamental diagram of urban networks, in: *Transportation Research Procedia, Papers selected for the International Symposium of Transportation and Traffic Theory (ISTTT)*, pp. 615–630.
- Laval, J.A., Chilukuri, B.R., 2014. The distribution of congestion on a class of stochastic kinematic wave models. *Transportation Science* 48, 217–224.
- Lebacque, J.P., 1996. The godunov scheme and what it means for first order traffic flow models, in: *International Symposium on Transportation and Traffic Theory (ISTTT)*, pp. 647–677.
- Lebacque, J.P., 2005. First-order macroscopic traffic flow models: Intersection modeling, network modeling, in: *Transportation and Traffic Theory. Flow, Dynamics and Human Interaction. 16th International Symposium on Transportation and Traffic Theory (ISTTT)*, pp. 365–386.
- Lu, J., 2020. Probabilistic models and optimization algorithms for large-scale transportation problems. Ph.D. thesis. Massachusetts Institute of Technology.
- Lu, J., Osorio, C., 2018. A probabilistic traffic-theoretic network loading model suitable for large-scale network analysis. *Transportation Science* 52, 1509–1530.
- MATLAB, 2016. *Optimization Toolbox: User’s Guide (R2016a)*. The Mathworks, Inc.. Natick, Massachusetts.
- Newell, G., 1993. A simplified theory of kinematic waves in highway traffic, part I: general theory. *Transportation Research Part B* 27, 281–287.
- Olszewski, P.S., 1994. Modeling probability distribution of delay at signalized intersections. *Journal of Advanced Transportation* 28, 253–274.
- Osorio, C., 2010. Mitigating network congestion: analytical models, optimization methods and their applications. Ph.D. thesis. Ecole Polytechnique Fédérale de Lausanne.
- Osorio, C., Bierlaire, M., 2009. An analytic finite capacity queueing network model capturing the propagation of congestion and blocking. *European Journal of Operational Research* 196, 996–1007.
Available at: <http://web.mit.edu/osorioc/www/papers/osoBie09EJOR.pdf> .
- Osorio, C., Chen, X., Gao, J., Talas, M., Marsico, M., 2016. A scalable algorithm for the control of congested urban networks with intricate traffic patterns: New York City case studies. Technical Report. Department of Civil and Environmental Engineering, Massachusetts Institute of Technology (MIT).
Available at: <http://web.mit.edu/osorioc/www/papers/osoCheNycdotQbbMtm.pdf> .

- Osorio, C., Flötteröd, G., 2015. Capturing dependency among link boundaries in a stochastic dynamic network loading model. *Transportation Science* 49, 420–431.
- Osorio, C., Flötteröd, G., Bierlaire, M., 2011. Dynamic network loading: a stochastic differentiable model that derives link state distributions. *Transportation Research Part B* 45, 1410–1423.
- Osorio, C., Wang, C., 2017. On the analytical approximation of joint aggregate queue-length distributions for traffic networks: A stationary finite capacity Markovian network approach. *Transportation Research Part B: Methodological* 95, 305–339.
- Osorio, C., Yamani, J., 2017. Analytical and scalable analysis of transient tandem Markovian finite capacity queueing networks. *Transportation Science* 51, 823–840.
- Smits, E.S., Bliemer, M.C., Pel, A.J., van Arem, B., 2015. A family of macroscopic node models. *Transportation Research Part B: Methodological* 74, 20–39.
- Stafford, R., 2006. The theory behind the 'randfixedsum' function. URL: [Http://www.mathworks.com/matlabcentral/fileexchange/9700](http://www.mathworks.com/matlabcentral/fileexchange/9700).
- Sumalee, A., Zhong, R.X., Pan, T.L., Szeto, W.Y., 2011. Stochastic cell transmission model (SCTM): a stochastic dynamic traffic model for traffic state surveillance and assignment. *Transportation Research Part B* 45, 507–533.
- Tampère, C., Corthout, R., Cattrysse, D., Immers, L., 2011a. A generic class of first order node models for dynamic macroscopic simulations of traffic flows. *Transportation Research Part B* 45, 289–309.
- Tampère, C.M., Corthout, R., Cattrysse, D., Immers, L.H., 2011b. A generic class of first order node models for dynamic macroscopic simulation of traffic flows. *Transportation Research Part B: Methodological* 45, 289–309.
- TSS, 2014. AIMSUN 8.1 Microsimulator Users Manual. Transport Simulation System.
- Viti, F., Van Zuylen, H.J., 2010. Probabilistic models for queues at fixed control signals. *Transportation Research Part B* 44, 120–135.
- Yperman, I., Tampere, C., Immers, B., 2007. A kinematic wave dynamic network loading model including intersection delays, in: *Transportation Research Board Annual Meeting*, Washington DC, USA.